Microwave analysis of MSM photodiodes for time-resolved measurements of RSFQ pulses

Siham Badi, Pascal Febvre

Microwave analysis of MSM photodiodes for time-resolved measurements of RSFQ pulses

Siham Badi† and Pascal Febvre†

† Microwave and Characterization Laboratory (LAHC) - University of Savoie, 73376 Le Bourget du Lac, France

E-mail: siham.badi@univ-savoie.fr

Abstract. This paper deals with a study of Metal-Semiconductor-Metal (MSM) photodetectors used for time-resolved detection of low amplitude picosecond-range signals, such as Rapid Single Flux Quantum (RSFQ) pulses [1] generated by superconductive electronics circuits. A typical 6ps-wide incoming RSFQ pulse of 200μV amplitude has been used for the analysis. The photodetector detection behaviour has been studied in the microwave frequency range for different geometrical parameters in the OFF (no optical illumination) and ON modes. It is shown that, with properly chosen geometry, the photoswitches exhibit good transmission of RSFQ pulses in the ON mode while reasonably shorting them in the OFF mode.

PACS numbers: 78.47.+p, 85.25.Hv, 85.60.Bt, 85.60.Dw

Submitted to: *Semicond. Sci. Technol.*

1. Introduction

With their high intrinsic speed of several tens of GHz and very low dissipation, superconductive circuits open the way to high-speed digital electronics. In Rapid Single Flux Quantum (RSFQ) digital circuits, based on shunted Josephson junctions, digital data are transmitted through picosecond voltage pulses with quantized area of 2.07 mV×ps, corresponding to one magnetic flux quantum. Hence, the pulse voltage is weak, of the order of 1 mV or less. Since this technology exhibits some unparallel performances for miscellaneous high-speed applications, it becomes valuable to be able to measure in a time-resolved manner the shape of digital signals coming out of RSFQ circuits, for diagnosis and for studying in detail the cause of their speed limits. To do so, ultrafast optoelectronics interfaces, triggered by a pulsed femtosecond Ti-Sa laser, are studied as readout of RSFQ signals. To date, SFQ pulses have been directly observed using an Electro-Optical (EO) sampling technique[2, 3, 4]. Measurements were based on an optoelectronic superconducting Niobium circuit consisting of a Nb-Si-Nb MSM photodiode, used as electrical signal generator, coupled to a microstrip line and connected to a two-junction pulse shaper followed by a coplanar line. The superconducting circuit has been entirely covered with an electro-optical lithium tantalate ($LiTaO_3$) crystal. The EO sampling setup reached a 200fs time resolution associated to a voltage resolution of about 100μV [2]. In its cryogenic version, the implementation of EO sampling technique is difficult to master in terms of alignments required between the device under test and both switching and sampling laser beams. Moreover, the necessity to grow a thin film of crystal on superconducting circuits puts additional steps and difficulties during the technological fabrication process.

Another method, based on photoconductive measurements, provides a possibility to detect weak RSFQ pulses. This method is based on Metal-Semiconductor-Metal (MSM) photodetectors [5] which consist of interdigitated metallic fingers deposited over a photosensitive semiconducting substrate. Their planar structure provides high response speed and good compatibility with other devices, in term of process fabrication and integration. Physical characteristics of semiconductor material such as dark resistivity, free carrier mobility and life time are the key parameters to obtain ultrashort pulses. Gallium arsenide materials grown at low temperature (LT-GaAs), are usually considered as favorable candidates for ultra-fast optoelectronics applications [6, 7] since a good time resolution is insured by the physical properties of the material [8]. In particular, Be-doped LT-GaAs materials present a high electron mobility (540 $cm^2/V/s$) and an ultra-fast electron lifetime (560 fs)[9]. For detection of ultrashort picosecond signals, the geometry of the photodetectors has to be optimized as well, in order to achieve a high detection sensitivity. In this work, we focus our attention on determining the microwave response of photodetectors and optimizing the MSM photodetector sensitivity accordingly, to be suitable to detect weak pulsed signals. First the microwave model of the photoswitch is described under and without optical illumination. In a second step, the scattering parameters for different photodetector geometries are

determined. In a last step, the reflected and transmitted waves and associated voltages in the ON and OFF modes are computed.

2. Microwave model

An example of interdigitated MSM photoswitch to be used for time-resolved readout of RSFQ circuits is shown in Fig.1. In order to measure picosecond RSFQ signals with a good time resolution, the sensitivity of the photodetector has to be optimized. To do so, a microwave analysis is necessary in the frequency range corresponding to the one of the signals to be measured. In a first step, the scattering parameters of photoswitches of different geometrical sizes, based on gallium arsenide substrates, have been calculated with ANSOFT Designer [10]. Then, to ease the analysis and extract pertinent parameters, a lumped element pi model, proposed in [11], is used to predict the behavior of the photoswitch when there is no applied optical illumination (OFF mode). The pi-model, shown in Fig.2-a, accounting for the interdigitated coplanar structure, is associated to C_g, C_p1 and C_p2 capacitances. This model has shown to be in quite good agreement with experimental results up to 25 GHz for a properly chosen geometry. See in particular Fig.16 of [11]. Following the work of [11], the geometry of the photoswitches has been modified in order to obtain good performances up to 200 GHz. To do so, the values of the capacitances have been computed by matching, in the frequency range of interest and for every photoswitch under study, the S-parameters obtained with ANSOFT Designer with the ones calculated from the S-matrix expressions associated to the pi-model. In practice, the three capacitances of the pi-model are expressed as a function of the S-parameters, derived from the ABCD-parameters. Then, the S-parameters computed by Ansoft Designer from the photo-switch geometry are fed in the expressions of the capacitances. The result is a set of capacitances for every frequency under study. At this point, the appropriateness of the pi-model is insured by the fact that the calculated capacitances are constant, within a few percents, over the whole frequency range of interest for our study, i.e. $0 - 200GHz$. In a last step, the S-parameters of the pi-model are directly computed from the obtained values of the capacitances, and compared with their Ansoft Designer counterparts. Associated Smith charts, along with scattering parameters magnitudes and phases are shown in Fig.3 for a photoswitch comprising five 40 μm-long, 8.75 μm-wide fingers spaced by a 1 μm gap.

Under illumination, the gap between the electrodes becomes conductive via photogeneration of carriers. Indeed, the absorption of incoming photons excites electrons and generates free carriers which exhibit a conductivity connected to their mobility in the material. Therefore the photoswitch is equivalent to a photovarying resistance R(t) that is in parallel with C_g (see Fig.2-b). We assumed that the resistance remains constant over time when the RSFQ pulse is present through the photoswitch, as a first approximation to determine the photoswitch response. This corresponds to the minimum of photovarying resistance, obtained for maximum optical illumination over the photoswitch (ON mode). To analyze the microwave behavior of the photoswitch,

it has been assumed, that the photoswitch is electrically fed by the RSFQ signal to be detected, coming from shunted Josephson junctions. For this study, we used a typical theoretical RSFQ pulse, for which the time–dependent pulse voltage is given in Eq.1 [13, 14], with a 6 ps Full-Width at Half-Maximum (FWHM) that corresponds to an amplitude of 0.22 mV since RSFQ pulses carry one quantum of magnetic field.

$$V(t) = V_c \frac{\omega^2}{i + cos(2\pi(\frac{2e}{h}V_c\omega)t)} \tag{1}$$

where $i = \frac{I_{bias}}{I_c}$, $\omega = \sqrt{i^2 - 1}$ and $V_c = R_n I_c$. I_c is the critical current of the shunted Josephson junction generating the RSFQ pulse, while I_{bias} is the bias current of this junction and R_n is the shunt resistance. The area of the pulse shown in Fig.4-a is constant: it equals 2.07mV×ps. The power spectrum associated to the RSFQ pulse shape is shown in Fig.4-b. The frequency range shown in this figure has been used to perform the microwave analysis. In the ON mode, it has been assumed that the photoswitch is triggered by an optical pulse of about 100 fs duration at 800 nm wavelength. The applied optical power is 10 mW which corresponds to a constant photo-generated carrier density.

3. Influence of geometrical parameters

In order to optimize the sensitivity of detection, one needs to have a good ON/OFF contrast of the photoswitch: that means that the RSFQ signal should be transmitted with very low attenuation in the ON mode while the same signal should be totally reflected in the OFF mode. To do so, the scattering parameters have been analyzed, in both OFF and ON modes, versus three parameters: gap d between fingers, finger width w and finger length L. For the whole study, the ratio $\frac{l}{l+2s}$ of the coplanar line (see Fig.1) associated to the photoswitch has been held constant at 0.44 in order to maintain a 50 Ω characteristic impedance for loading the photoswitch with pulsed RSFQ signals. Consequently it is assumed that there is no reflected wave at the load and generator ports.

3.1. Electrical parameters R, Cg, C_p1 and C_p2

Electrical parameters (resistance R and capacitances Cg, Cp_1 and Cp_2) have been analyzed as a function of the photodetector geometrical parameters. The illuminated area of the photoswitch becomes conductive, which corresponds to a variable resistance depending on carriers density, hence on photons density. The photo-varying resistance can be described as follow:

$$R(t) = \frac{d}{qNLt(\mu_n n(t) + \mu_p p(t))} \tag{2}$$

where q is the charge of the electron, t is the depth over which the carriers are generated, μ_n and n(t) (μ_p and p(t)) are respectively the free electrons (holes) mobility and

concentration. d, N and L are respectively the gap between fingers, and the number and length of fingers of the photoswitch. Fig. 5 shows an example of photoswitch photo-varying resistance. The carrier concentrations n(t) and p(t) vary as the inverse of the lit area (L×d), due to the constant total applied optical power: this implies that the optical power density depends on the photoswitch geometry. As a consequence, the photo-resistance R(t) depends on the square of the activated zone of width d, as can be seen in Fig.6-a where the number of fingers N, the finger length L and finger width w have been respectively held at N = 5, L = 40 μm and w = 1 μm for different photoswitch gaps.

Regarding the gap capacitance C_g, a good approximation can be obtained with Eq(3) and Eq(4), where K is the complete elliptic integral of the first kind. C_g can be understood as the capacitance of a coplanar gap d whose width is the length N×l of the meander between electrodes. C_g is given versus the ratio $\frac{w}{w+d}$ in Fig.6-b for N = 5 and L = 40μm. In practice, this ratio is chosen in the linear part of the curve to minimize the influence on C_g of geometrical parameter variations .

$$C_g = NL\varepsilon_0(\varepsilon_r + 1)\frac{K(k)}{K(k')} \tag{3}$$

$$k = \frac{w}{w+d} \; ; \; k' = \sqrt{1-k^2} \tag{4}$$

Parasitic capacitances C_p1 and C_p2 of Fig.2 are connected to the capacitance per unit length of the coplanar transmission line of spacing s and center strip width l. A good approximation is given by Eq(5) and Eq(6). For a 50 Ω characteristic impedance, C_p1 and Cp_2 only depend on the finger length L: $C_p1 = C_p2 = 3.46$ fF for L = 40 μm.

$$C_{pi} = L\varepsilon_0(\varepsilon_r + 1)\frac{K(k_1)}{K(k_1')} \tag{5}$$

$$k_1 = \frac{l}{l+2s} \; ; \; k_1' = \sqrt{1-k_1^2} \tag{6}$$

3.2. Scattering parameters

Reflected and transmitted scattering parameters $S11$ and $S21$ have been computed from electrical parameters for different geometrical configurations of interdigitated MSM photodetectors. Fig.7-a shows the influence, in the OFF mode, of the gap d for photoswitches with fixed number of fingers, finger width and finger length. Fig.7-b shows similar curves when the photoswitch is illuminated (ON mode).

The Smith chart of $S11$ of Fig.7-a shows that the photoswitch has an OFF mode impedance close to the one of an open circuit in the whole frequency range of interest (e.g. up to 200 GHz). This means that, despite a non-negligeable phase for high frequencies, the incoming RSFQ pulses are well reflected for a wide range of finger spacings and frequencies, as long as the finger width is not too wide, as can be seen in the Smith chart of Fig.8-a. Nevertheless, $|S21|$ of Fig.7-a shows that only the upper

frequency part of the signal to detect can go through the photoswitch, which can be avoided in practice by increasing the gap d. Hence, when one only considers the OFF mode, a good reflection is obtained a priori for large gaps and narrow widths.

In the ON mode, the Smith chart of Fig.7-b shows that the impedance match is relatively good as long as the gap d is not too wide: the reflection coefficient is lower than $-11\ dB$ over the whole 200 GHz frequency range as long as the spacing is lower than $10\mu m$. In the worst case, for a spacing of $20\mu m$, the reflected power becomes significant, since the reflection coefficient reaches $-5.2\ dB$ at 200 GHz. This means that the spacing has to be kept below $10\mu m$, which we assume in the following. Also, under illumination, the scattering parameters do not depend on width, length and number of fingers for a fixed gap d. Indeed, the capacitance Cg is shunted by the resistance R that only depends on d. Hence, one can deduce that the main geometrical parameter that influences the photoswitch behavior in terms of sensitivity, under illumination, is the finger gap d which should be minimized to increase the signal transmission.

The above analysis implies that the optimum value of d is a trade-off between good transmission in the ON mode and low transmission in the OFF mode. One solution to bypass this trade-off is to minimize d to increase the signal transmission in the ON mode, while playing with the other parameters to minimize the transmission in the OFF mode. Fig.8 shows the scattering parameters in the OFF mode of a photoswitch with N = 5 fingers and a gap d = 10μm for different finger lengths L and finger widths w. It is deduced from this figure that a low transmission in the OFF mode is associated to short and narrow fingers.

In order to summarize and to give a general idea of the influence of the photoswitch geometrical parameters on scattering parameters in OFF and ON modes, we have computed reflection and transmission parameters for a fixed frequency versus finger gap d and width w while keeping constant at $20\mu m$ the width of the coplanar line center strip. At 200GHz, Fig.9 displays $S11$ and $S21$ in the OFF mode while Fig.10 shows the same parameters in the ON mode. The 3D plots are composed of several curves, corresponding to different number of fingers. Indeed, since the width l of the coplanar line is fixed, there is a relation of constraint between the spacing d and the width w through the number of fingers N, as can be seen in Fig.1. The relation can be expressed through the following equation (7):

$$l = Nw + (N-1)d \tag{7}$$

Fig.9 confirms the previous analysis and shows that a good signal reflection in OFF mode is obtained for wide spacings d and narrow finger widths w. On the other hand, in the ON mode, Fig.10 exhibits a good transmission for large widths w and narrow gaps d. As mentioned above, one chooses a narrow gap d for optimum signal transmission in the ON mode. Consequently, the associate finger width w is rather large. Nevertheless, for such a fixed narrow gap d, Fig.9 shows that the reflection in the OFF mode will be maximum for large widths, even if this reflection is not as good as the one obtained

by considering only the OFF mode for optimization. As a consequence, a clear trend for an optimized geometry of the photoswitches consists of using low d's and large w's. This implies that the number of fingers is low, according to equation (7). By pushing the analysis at the limit, a good geometry is simply the one of a coplanar gap (previous case with zero finger). Nevertheless, one should mention here that there is not a unique solution for optimized geometry since the trade-off between good transmission in ON mode and good reflection in OFF mode is obvious from the previous analysis.

4. Transmission of pulsed signals

For this study, it has been assumed that the photoswitch under consideration has five 40μm-long, 1μm-wide fingers. The power spectrum of reflected and transmitted waves, along with the associated pulse temporal shapes, are shown in Fig.11 and Fig.12 in the OFF mode and ON mode respectively. Several photoswitches of different gaps d have been considered. For these calculations, the incoming signal is the one shown in Fig.4-a.

These two figures confirm what has been deduced in the former paragraph, i.e. that a low gap d is associated to a good transmission in the ON mode of the signal to detect but also, unfortunately, to a good transmission when the switch is not illuminated. This effect will be even more noticeable for shorter signals carrying more energy at high frequencies. Nevertheless we note that the average signal amplitude in the ON mode is about four times as high as in the OFF mode, which corresponds to a reasonable contrast.

5. Conclusion and perspectives

The influence of different geometrical parameters of interdigitated MSM photodetectors has been studied in order to optimize their sensibility to measure weak ultrashort RSFQ signals. Finger width and length should be chosen in order to minimize the interdigitated capacitance C_g. For a given width of the coplanar line center strip accommodating the photoswitch, the finger width and gap have to be, respectively, maximized and minimized. Nevertheless, the photo-resistance has been considered constant over signal duration in this analysis. This is not the case in practice for very short signals. A deeper analysis is necessary to take into account the variation of the resistance over time in these cases.

6. Acknowledgment

The authors would like to thank J.-L. Coutaz, J.-F. Roux and H. Eusèbe from LAHC at University of Savoie for helpful discussions.

7. References

[1] Likharev K K and Semenov V K 1991 *IEEE Trans. Appl. Superconductivity* **1** 3–27

[2] Wang C, Currie M, Jacobs-Perkins D, Feldman M J, Sobolewski R and Hsiang T 1995 *Appl. Phys. Lett.* **66** 3325–27
[3] Sobolewski R 2001 *Supercond. Sci. Technol.* **14** 994–1000
[4] Adam R, Williams C, Sobolewski R, Harnack O and Darula M 1999 *Supercond. Sci. Technol.* **12** 912–14
[5] Liou L and Nabet B 1996 *Applied Optics* **35** 15–23
[6] Whitaker J F 1993 *Mater. Sci. Eng.* **B22** 61–67
[7] Nolte D D 1999 *J. Appl. Phys* **85(9)** 6259–89
[8] Coutaz J L 2002 *Proc. XXXI Int. School Semicond. Compounds, Acta Physica Polonica A* vol. 102, no 4–5 pp 495–512
[9] Eusèbe H, Roux J F, Coutaz J L and Krotkus A 2005 *J. Appl. Phys.* **98** 33711
[10] Ansoft Designer version 1.1 1998-2003 copyright (C) Ansoft
[11] Naghed M and Wolff I 1990 *IEEE Trans. Microwave Theory Tech* **38(12)** 1808–15
[12] Krotkus A, Bertulis K, Kaminska M, Korona K, Wolos A, Siegert J, Marcinkevicius S and Coutaz J L 2002 *IEE Proc. Optoelec.* **149(3)** 111–5
[13] Febvre P, Berthet J C, Ney D, Roussy A, Tao J, Angenieux G, Hadacek N, Villegier J C 2001 *IEEE Trans. Appl. Supercond.* **11(1)** 284–7
[14] Feldman M J 1999 *Phys. and Appl. of Mesoscopic Josephson Junctions* (ed H Ohta and C Ishii: Physical Society of Japan - Tokyo,) pp. 289-304

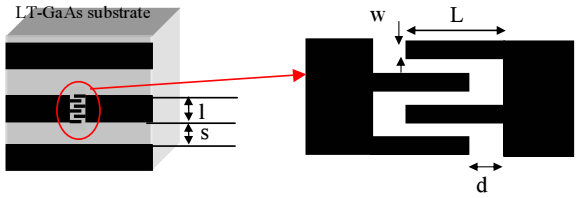

Figure 1. MSM photodetector configuration: gold electrodes are deposited on the LT-GaAs substrate. Parameters l, s, L and w can be adjusted, along with the number N of fingers.

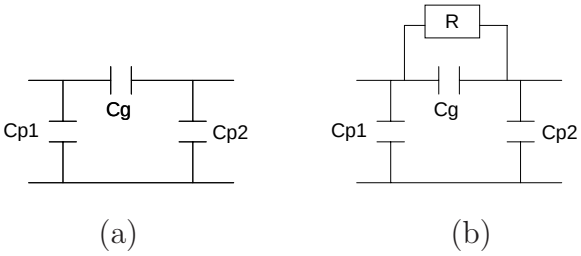

Figure 2. Pi-model of MSM photodetector (a) without illumination and, (b) under illumination.

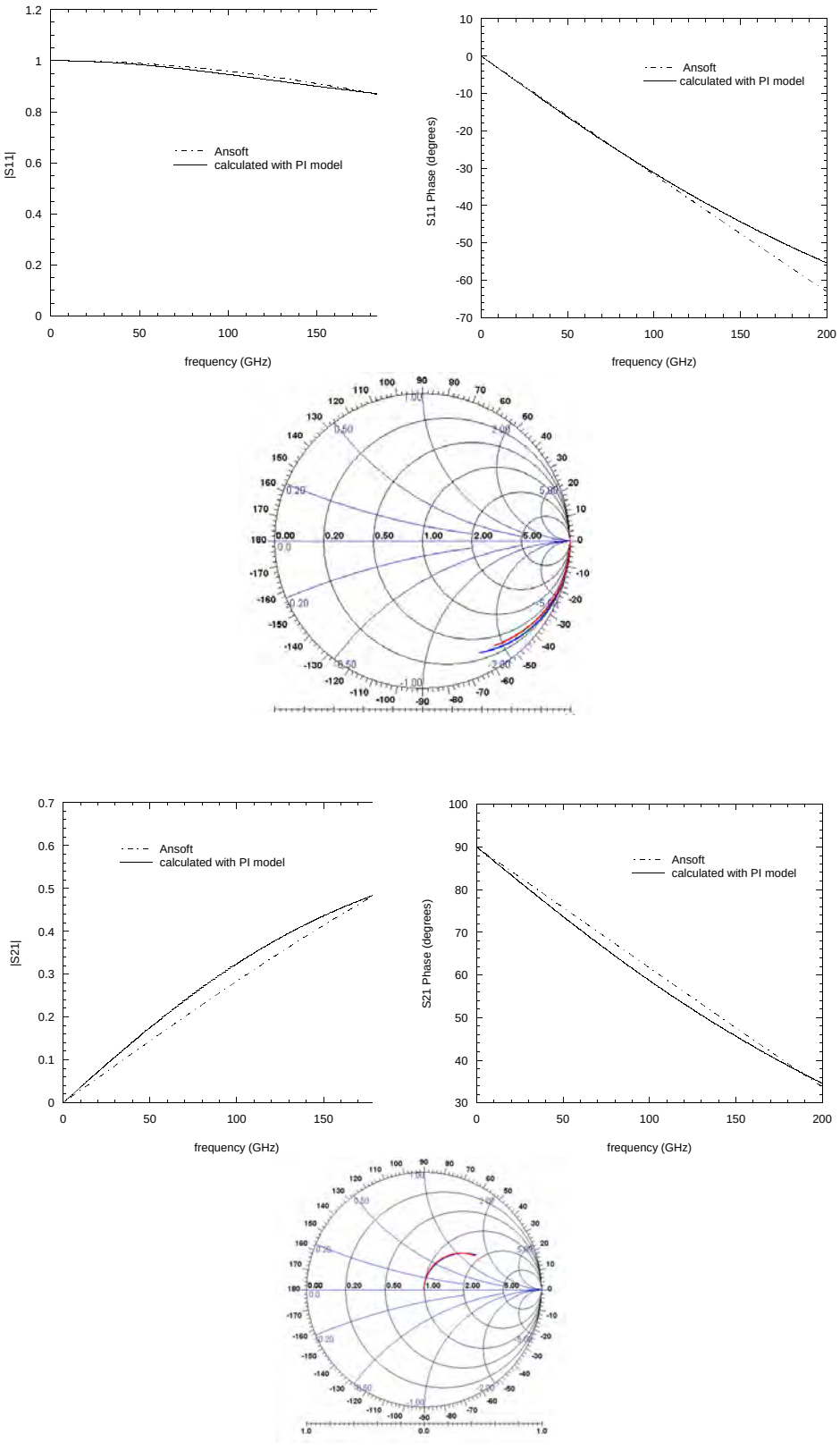

(b)

Figure 3. Scattering parameters magnitudes and phases, along with Smith charts, of (a)$S11$ and (b)$S21$ for an interdigitated photodetector in OFF mode (N = 5, L = 40μm, w = 8.75μm and d = 1μm), computed with Ansoft Designer and simulated with the pi-model.

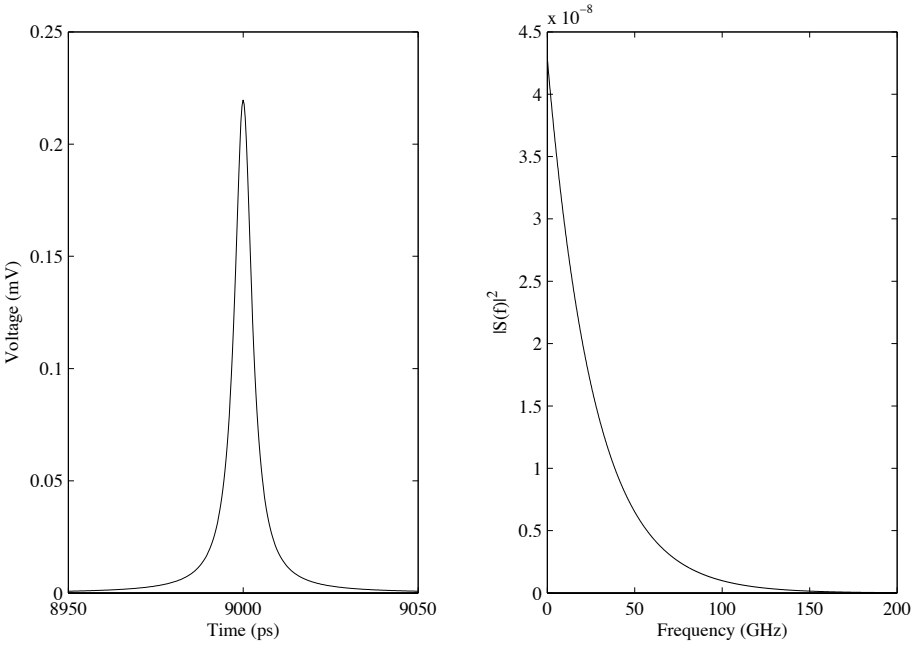

Figure 4. (a) RSFQ pulse generated by a shunted Josephson junction with FWHM = 6ps and $R_n\ I_c = 0.11$mV; (b) associated power spectrum.

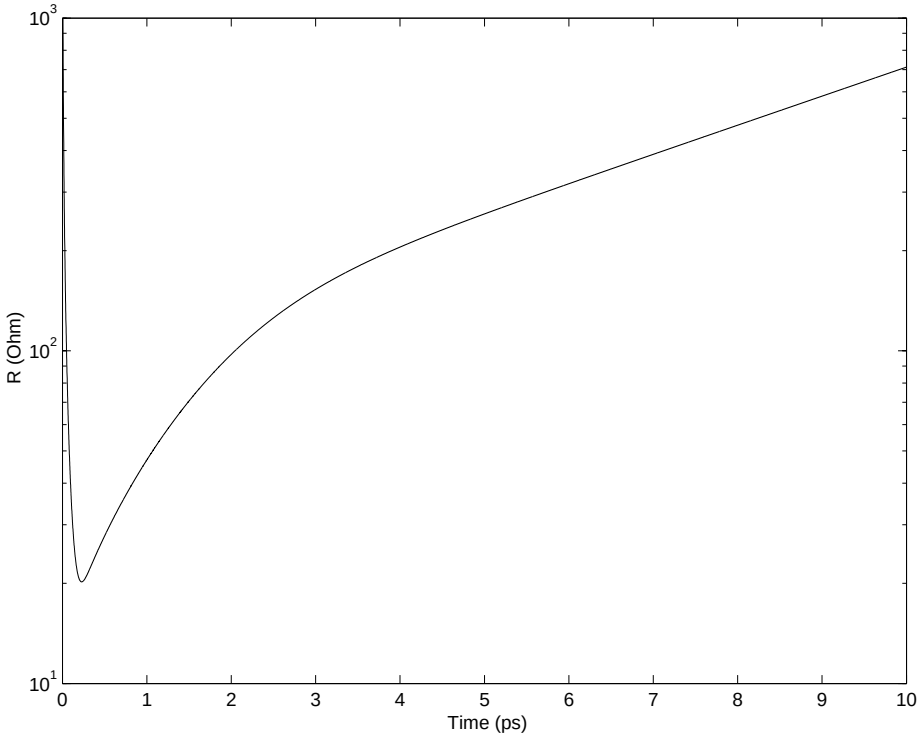

Figure 5. : Temporal variation of the photoswitch resistance under illumination. The geometrical parameters are: d=8.75μm, w=1μm, L=30μm, N=5. The photoswitch is excited by 100-fs optical pulses delivered by a pulsed Ti:Sa laser (wavelength of 800 nm) with a 10 mW average power, at a repetition rate of 82 MHz.

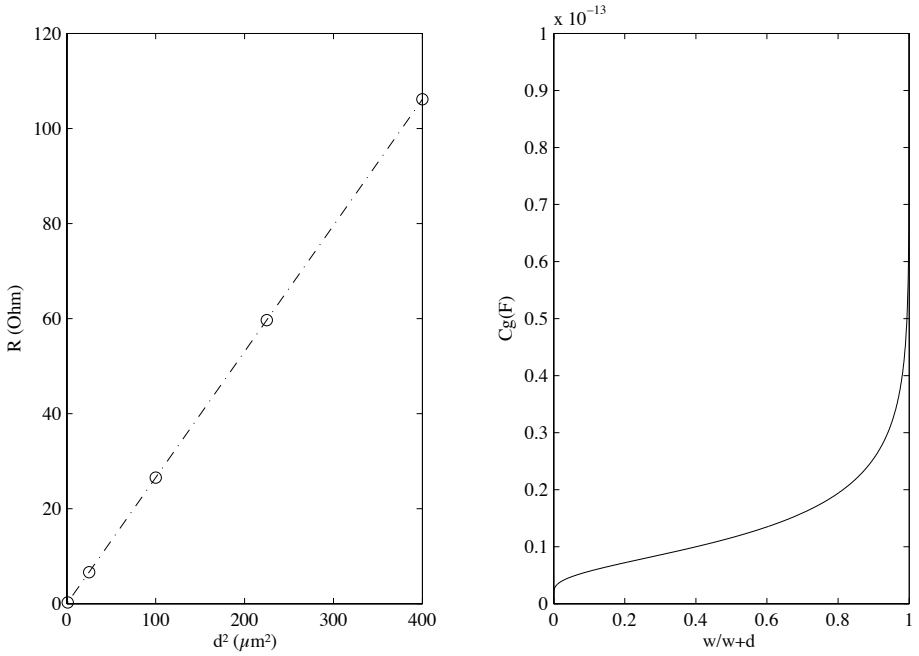

Figure 6. (a) Minimum of photovarying resistance under illumination versus the square of finger gap d. The interdigitated photodetector has N = 5 fingers with L = 40μm and w = 1μm; (b) Photoswitch gap capacitance Cg versus w/(w+d) for N = 5 and L = 40μm.

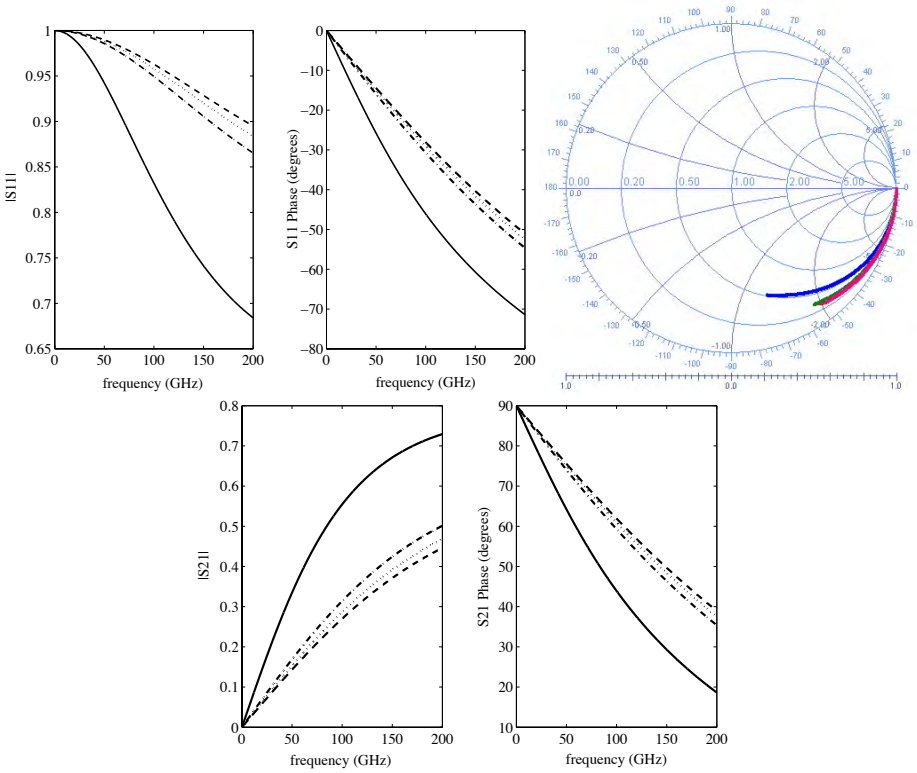

(a) without illumination (OFF mode)

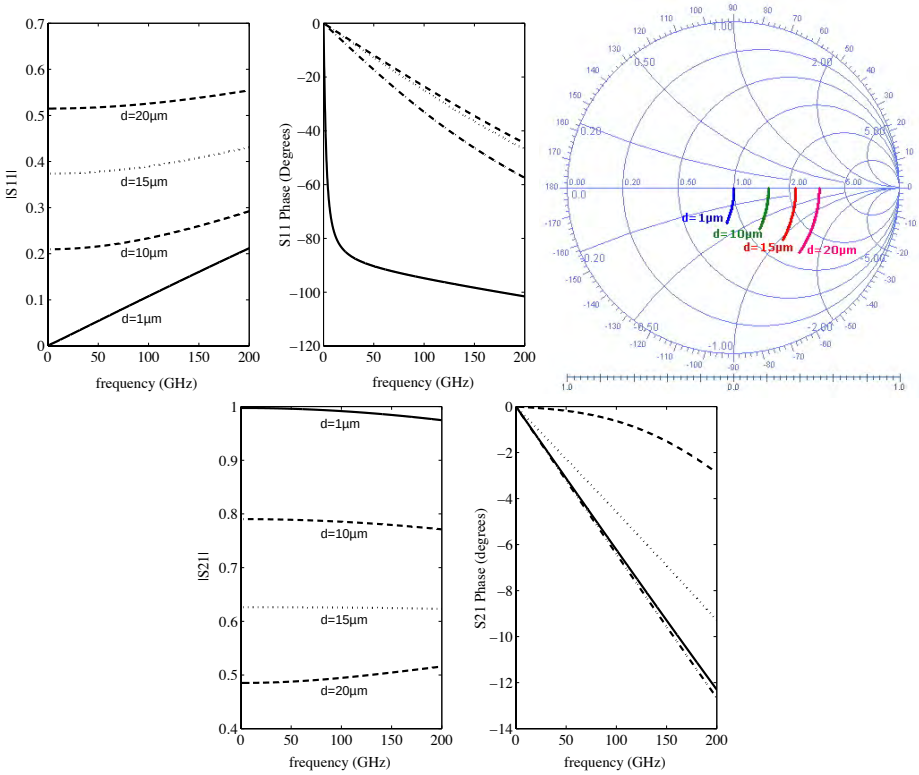

(b) under illumination (ON mode)

Figure 7. $S11$ (magnitude, phase and Smith chart) and $S21$ (magnitude and phase) of interdigitated photodetectors (N = 5, L = 40μm, w=1μm) for different gaps: d = 1μm (—); d = 10μm (– · –); d = 15μm (· · ·) and d = 20μm (- -).

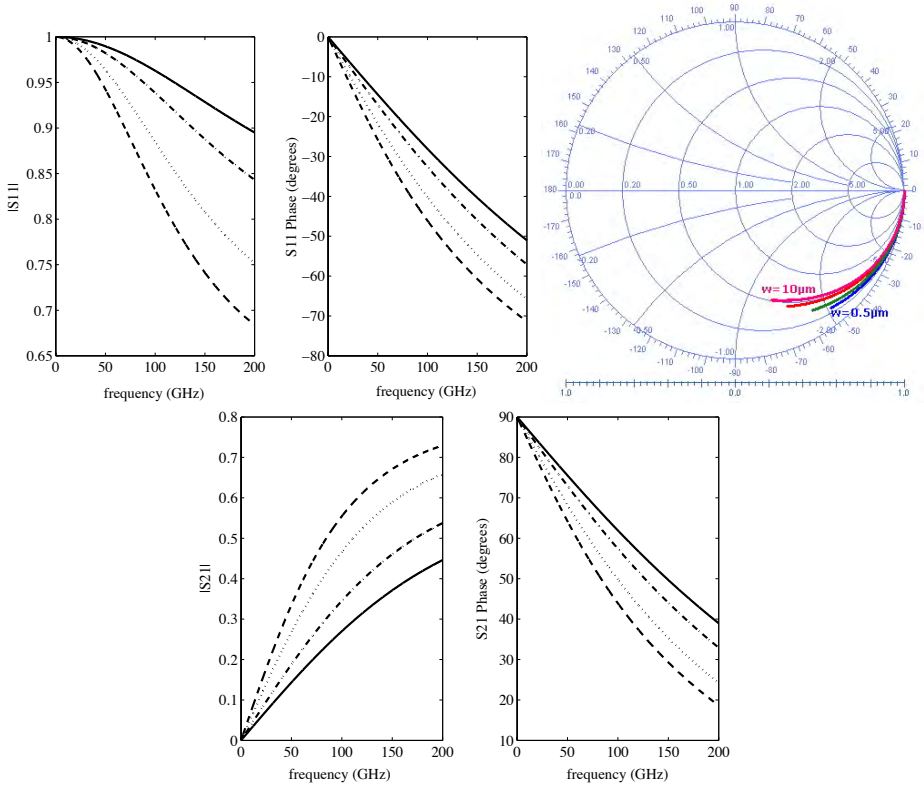

(a) influence of finger width w in OFF mode

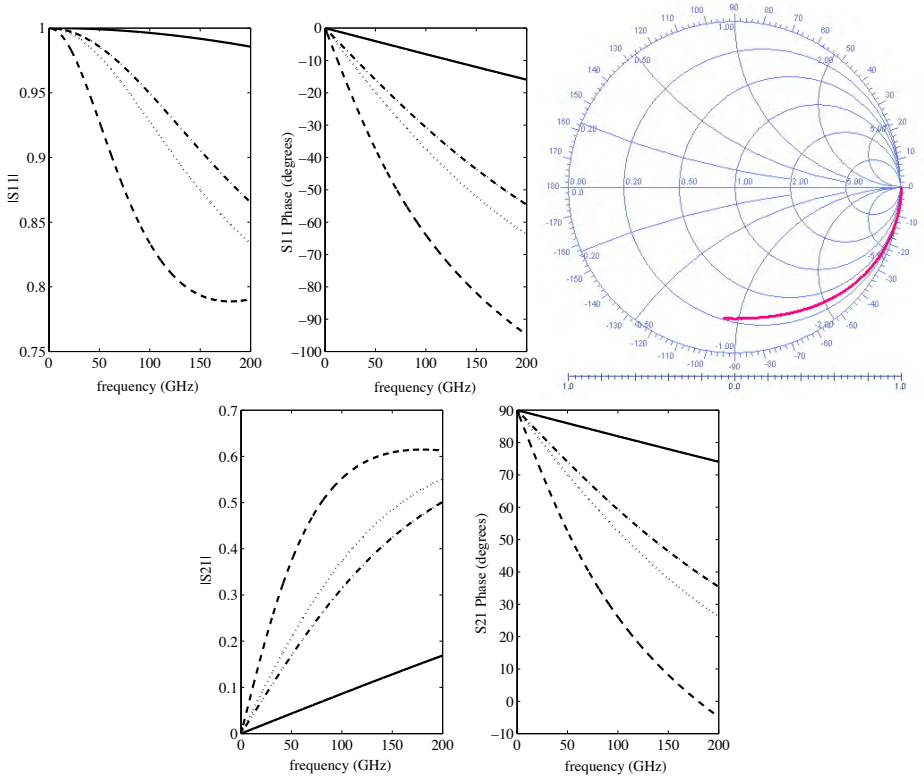

(b) influence of finger length L in OFF mode

Figure 8. : $S11$ (magnitude, phase and Smith chart) and $S21$ (magnitude and phase) of interdigitated photoswitches with N = 5 fingers with gap d = 10μm in the OFF mode for: (a) different finger widths: w = 0.5μm (—); w = 1.5μm (– · –); w = 4μm (····) and w = 10μm (- -) with L = 40μm and for: (b) different finger lengths: L=10μm (—); L = 40μm (– · –); L = 50μm (· · ·) and L=100μm (- -) with w = 1μm.

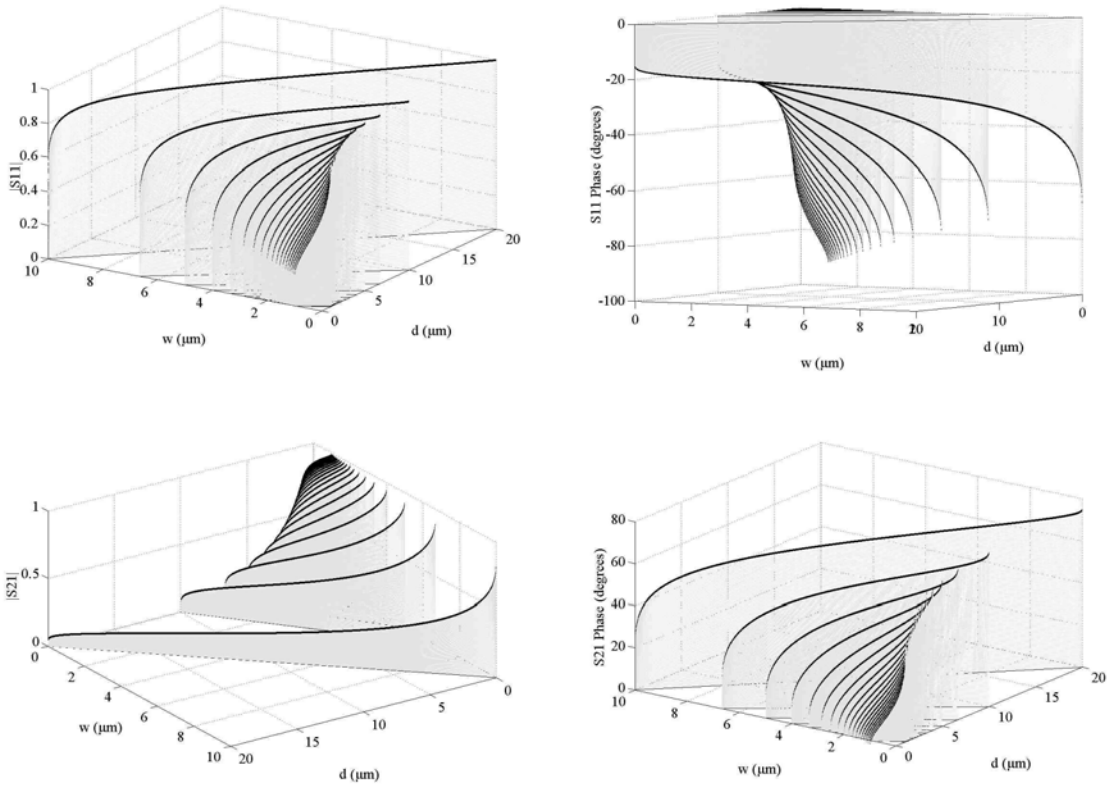

Figure 9. : Finger gap(d) and width(w) dependence of $S11$ and $S21$(magnitude and phase) for photoswitches without illumination with L = 20μm with a coplanar line center strip width fixed at 20 μm. This study is done at a fixed frequency at 200GHz. The vertical planes, located below the bold lines, along with the thin solid lines in the (w,d) plane are a guide for the eye.

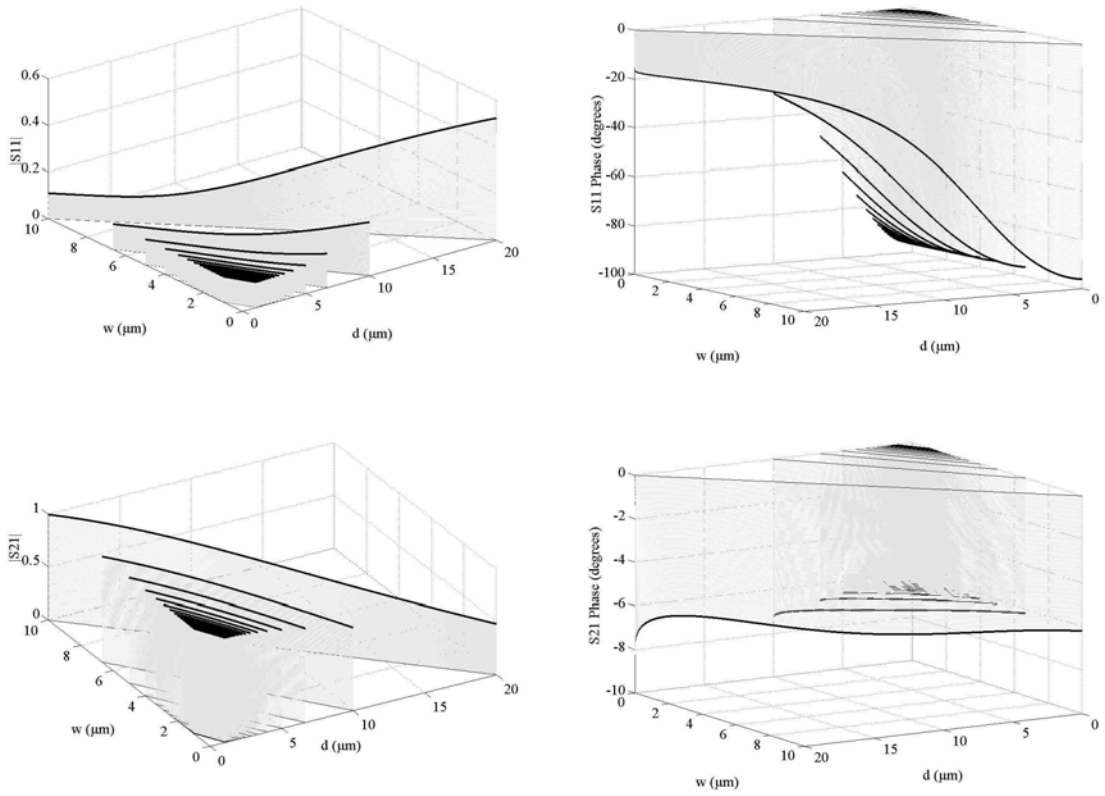

Figure 10. : Magnitude and phase of $S11$ and $S21$ versus finger gap(d) and width(w) for illuminated photoswitches with L = 20μm with a coplanar line center strip width fixed at 20 μm. This study is done at a fixed frequency at 200GHz. The vertical planes, located below the bold lines, along with the thin solid lines in the (w,d) plane are a guide for the eye.

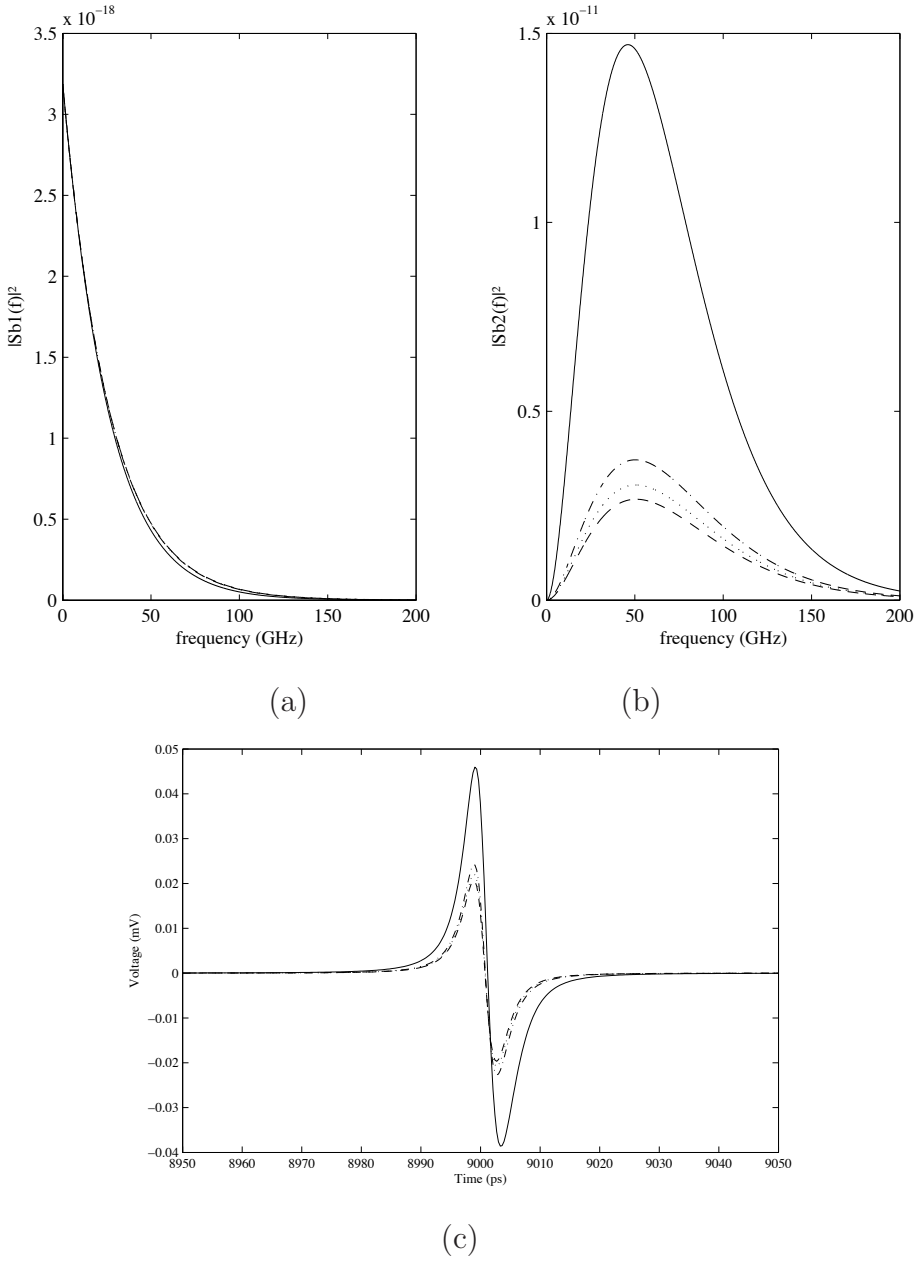

Figure 11. : Power spectrum in the OFF mode of (a) reflected and (b) transmitted wave for a photoswitch with N = 5, L = 40μm and w = 1μm; (c) Photodetector output voltage in the time domain. Different gaps d have been considered: d = 1μm (—); d = 10μm (– · –); d = 15μm (· · ·) and d = 20μm (- -).

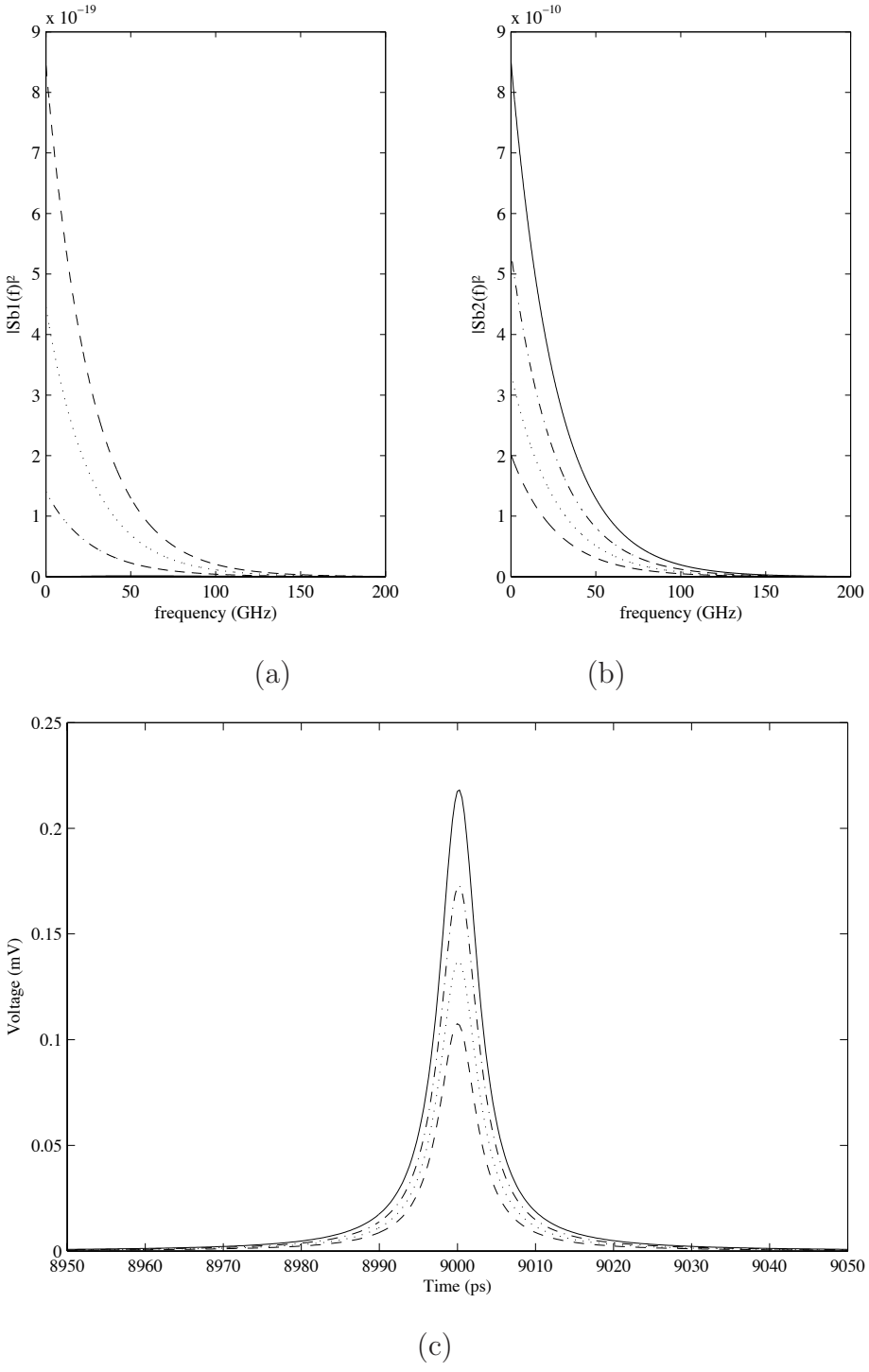

Figure 12. : Power spectrum in the ON mode of (a) reflected and (b) transmitted wave for a photoswitch with N = 5, L = 40μm and w = 1μm; (c) Photodetector output voltage in the time domain. Different gaps d have been considered: d = 1μm (—); d = 10μm (– · –); d = 15μm (· · ·) and d = 20μm (- -).